The comparison of OpenCV library algorithms for tracking movements of liver tumors in ultrasound video.

Alexander A. Levin (alex.levin@internet.ru)
Moscow State University of Medicine and Dentistry
Daniil D. Klimov
Moscow State University of Medicine and Dentistry
Alexey A. Nechunaev
Moscow State University of Medicine and Dentistry
Leonid S. Prokhorenko
Moscow State University of Medicine and Dentistry
Denis S. Mishchenkov
Moscow State University of Medicine and Dentistry
Anastasia G. Nosova
Moscow State University of Medicine and Dentistry
Dmitriy A. Astakhov
Moscow State University of Medicine and Dentistry
Yuri V. Poduraev
Moscow State Technological University
Dmitry N. Panchenkov
Moscow State University of Medicine and Dentistry

Research Article

Keywords: ultrasound, radio-frequency ablation, biopsy, liver tumor, robot-assisted surgery, computer vision, object tracking, opencv

Posted Date: February 15th, 2022

DOI: https://doi.org/10.21203/rs.3.rs-1359182/v1

Additional Declarations: Competing interest reported. There is potential Competing Interest. Support by the Ministry of Health of the Russian Federation in the framework of the State Contract No. 056-00035-21-00 of December 17, 2020.

Version of Record: A version of this preprint was published at Scientific Reports on April 25th, 2023. See the published version at https://doi.org/10.1038/s41598-023-30930-3.

Abstract

This study aims to compare the tracking algorithms provided by the OpenCV library to use on ultrasound video. Despite the widespread application of this computer vision library, few works describe the attempts to use it to track the movement of liver tumors on ultrasound video.

Movements of the neoplasms caused by the patient`s breath interfere with the positioning of the instruments during the process of biopsy and radio-frequency ablation. The main hypothesis of the experiment was that tracking neoplasms and correcting the position of the manipulator in case of using robotic-assisted surgery will allow positioning the instruments more precisely. Another goal of the experiment was to check if it is possible to ensure real-time tracking with at least 25 processed frames per second.

OpenCV version 4.5.0 was used with 7 tracking algorithms from the extra modules package. They are: Boosting, CSRT, KCF, MedianFlow, MIL, MOSSE, TLD. More than 4900 frames of standard definition were processed during the experiment.

Analysis of the results shows that two algorithms – CSRT and KCF – could solve the problem of tumor tracking. They lead the test with more than 70% of ROI coverage and more than 95% successful searches. They could also be used in real-time processing with an average processing speed of up to 30 frames per second in CSRT and up to 100 frames per second for KCF.

This experiment also shows that no frames made CSRT and KCF algorithms fail simultaneously. So, the hypothesis for future work is combining these algorithms to work together, with one of them – CSRT – as support for the KCF tracker on the rarely failed frames.

Introduction

Neoplasms detected in the human liver are quite diverse. They can be parasitic invasions – echinococcus or alveococcus, non-parasitic cysts – both solitary and multiple, including those caused by polycystic disease, liver abscesses and inflammatory pseudotumors, liver tumors **[1].** Tumors can be benign or malignant. Malignant tumors, in turn, can be primary – hepatocellular or cholangiocellular cancer and metastatic – colorectal metastases, metastases of pancreatic cancer, lung cancer, breast cancer, stomach cancer **[2].**

A liver adenoma is a benign liver tumor that occurs in 1 case in a million cases. An incidence increase was noted in women receiving oral contraceptives **[3].** Measuring less than 5 cm, liver adenomas, for the most part, do not have specific symptoms. Focal nodular hyperplasia refers to hamartomas and is associated with congenital or acquired vascular malformations leading to hepatocyte hyperplasia. It has an asymptomatic course with a size of less than 5 cm. Iso- or hypoechoic formation during Doppler scanning, which makes it possible to find a central supply vessel, diverging in the form of a spoked wheel to the periphery **[3].** Diagnosis of simple liver cysts is not so difficult. They usually occur in women 50+ years and are fluid formations that are well detected by ultrasound, CT, or MRI **[1].** Biliary cystadenomas are similar in their histological structure to mucinous adenomas of the pancreas and differ from simple liver cysts by the presence of septa, layering, papillary protrusions, and calcification. The most common liver formations are hemangiomas, up to 20% of the total population. Hemangiomas have a specific ultrasound or CT-MRI structure with a characteristic accumulation of contrast **[4].**

Abscesses are secondary cystic lesions of the liver. As a rule, they are associated with biliary infections accompanying obstruction of the biliary tract or manipulation of the bile ducts or parasite infestations **[5].**

Primary liver cancer ranks 5th in the incidence of malignant neoplasms in the United States with a 5-year survival rate of 20%; colorectal cancer ranks 3rd, while mortality from it is also in 3rd place in the structure of malignant neoplasms **[6].** This can be explained by the fact that 20% of initially diagnosed cases are determined already at the 4th stage with liver metastases **[7].** In gastric cancer, the diagnosis of the disease at the 4th stage is noted in one third of all cases **[8],** while liver metastases in these patients were noted in 41.30% **[9].** It is also significant that the frequency of metastasis of various malignant neoplasms depends on age. The most common source of liver metastases is breast cancer for women aged 20 to 50 and colorectal cancer for men. As patients get older, a more heterogeneous group of cancers with liver metastases emerges, including cancers of the esophagus, stomach, small intestine, melanoma, bladder cancer, in addition to a significant proportion of lung and pancreatic cancers. The 1-year survival rate of all patients with liver metastases is 15.1% compared to 24.0% in patients with non-liver metastases. Regression analysis showed that the presence of liver metastases causes a decrease in survival, especially in patients with cancer of the testicles, prostate, breast, and anus, as well as in patients with melanoma **[10].**

In recent years, minimally invasive surgery has become the standard in cancer treatment **[11].** It reduces the period of hospitalization and postoperative recovery. Modern minimally invasive surgery also implies the widespread use of technological advances such as robotic manipulators **[12],** computer vision systems **[13],** and artificial intelligence **[14].** Modern research spot, that using robotic systems for carrying out minimally invasive surgical procedures significantly increases their quality and efficiency **[15]**. In particular, this is due to the fact that modern robotic systems can achieve higher accuracy parameters than allowed by natural human systems.

Minimally invasive ultrasound-guided interventions can be divided into diagnostic, therapeutic-diagnostic, and therapeutic groups. Diagnostic ones include biopsies of liver tumors, taking fluid from the cavities of the cysts to clarify the diagnosis. Treatment and diagnostic include manipulations when the diagnostic stage immediately precedes the treatment. Therapeutic measures include various manipulations aimed at cure process – drainage of abscesses, bile ducts if they are obstructed, methods of local destruction of liver tumors, such as radiofrequency ablation (RFA), cryoablation, microwave ablation (MVA), irreversible electroporation of tumors. These interventions require high precision during the operation phase. Firstly, due to the determination of safe access to the dilated duct, tumor, or cyst and also to the fact that therapeutic effects on liver tumors may be accompanied by thermal damage. This requires precision installation of the working parts of the electrodes, avoiding close contact with the vascular and secretory structures of the liver **[16].**

Movements and deformations of the abdominal organs caused by breathing and other processes lead to a deviation of the neoplasm's target position from the preliminary plan of the operation based on CT or MRI data. Thus, in the case of using robotic systems in minimally invasive surgery, there is a need for intraoperative navigation, which can provide real-time data of the target's position for automated control of the medical instrument.

One of the simplest and most common methods of intraoperative visualization of the abdominal organs is ultrasound diagnostic. Its main advantage over intraoperative computed tomography and magnetic resonance imaging is greater availability due to a lower price. For example, the cost of an intraoperative MRI device from leading European manufacturers exceeds a million € while ultrasound devices, which by their characteristics allow

solving such problems, have ten times less cost. Also, in comparison with computed tomography, it does not adversely affect the patient and operating personnel. This can be very important in cases of long-term operations. However, it should be noted that ultrasound images are often inferior in quality of computed tomography due to the deterioration or lack of clear visualization of tissues caused by ultrasound artifacts which can negatively impact the interpretation of the results. The detection and dynamics of neoplasms using ultrasound are not an easy task for medical practitioners. Applying modern computer vision technologies could reduce the labor costs of medical personnel and possibly increase the accuracy of determining the center of neoplasms needed for real-time navigation of robotic manipulators for such operations as biopsy and radiofrequency ablation.

The main goal of this work was to test publicly available algorithms for tracking objects within an ultrasounds video. Both quality and performance were investigated.

The OpenCV library is the standard for developing computer vision applications. This project was launched in 1999 by the research division of Intel Corporation. For more than 20 years of development, the library has been replenished with many modules that find their application in such areas as face and gesture recognition, robotics, objects detection and segmentation in an image, augmented reality, and many others. This library is open-source software licensed under the Apache 2.0 License. Another reason for choosing OpenCV was the support for a tracking module with a wide variety of different algorithms, high-quality documentation, and a large user community.

Since the OpenCV library is widely used in many areas, the community created certain photo and video data sets to analyze the quality and speed of included algorithms **[17].** In particular, there are data sets for testing tracking algorithms **[18].** Usually, these sets include various objects of the real world (people, animals, objects) captured on video with variable quality (presence of noise, insufficient illumination etc.). However, most researchers and programmers widely use such sets that do not contain specific data like ultrasound video images.

Design and Methods

OpenCV library version 4.5.0 **[19]** was used for the experiment. It was compiled from source code with additional modules support **[20]**, including the tracking module. The following algorithms of this module were tested:

• Boosting – based on AdaBoost algorithm with HAAR cascade detector. The main idea of online boosting is the introduction of the so-called selectors. They are randomly initialized, and each of them holds a separate feature pool of weak classifiers. When a new training sample arrives, the weak classifiers of each selector are updated. The best weak classifier (having the lowest error) is selected, where the error of the weak classifier is estimated from samples seen so far **[21]**.

• MIL – a tracker that is similar to Boosting but also uses a small area around the tracker's current location **[22]**.

• KCF – a tracker based on the fact that the positive samples used in the MIL tracker have large overlapping regions. Processing these regions allows to simultaneously increase the speed and accuracy of tracking **[23]**.

• CSRT – Correlation Filter with Channel and Spatial Reliability. The spatial reliability map adapts the filter support to the object suitable for tracking, which overcomes both the problems of circular shift enabling an arbitrary search range and the limitations related to the rectangular shape assumption. The spatial reliability map is estimated using the output of a graph labeling problem solved efficiently in each frame **[24]**.

• MOSSE is a tracker based upon the Minimum Output Sum of Squared Error filter, robust to variations in lighting, scale, and deformations. It can pause and resume when the object is left off and appears again **[25]**.

• MedianFlow – the main idea is tracking points inside a bounding box by Lucas-Kanade tracker, which generates a sparse motion flow between Image N and Image N+1. The quality of the point predictions is estimated, and each point is assigned an error. The worst 50% of the predictions are filtered out, while the remaining predictions are used to estimate the displacement of the whole bounding box **[26]**.

• TLD – Tracking-Learning-Detection – a framework designed for long-term tracking of an unknown object in a video stream. Tracker estimates the object's motion between consecutive frames under the assumption that the frame-to-frame motion is limited, and the object is visible. The tracker is likely to fail and never recover if the object moves out of the camera view. The detector treats every frame as independent and performs full scanning of the image to localize all appearances that have been observed and learned in the past. Learning monitors the performance of both tracker and detector, estimates detector errors, and generates training examples to avoid these errors in the future **[27]**.

Despite attempts to apply supervised machine learning methods to solve this problem **[28]**, such experiments require many video files with reference labeling. This is one of the further works for applying artificial intelligence algorithms for ultrasound video processing. This work considers only the built-in algorithms of the OpenCV library.

In addition, the problem of real-time tracking is often solved by reducing the image fed to the tracking functions with the subsequent restoration of the original size **[29]**, which is primarily caused by low performance, especially when processing HD images. This technology is not used for the experiment – the frames of the original size frames are examined since a hypothesis is put forward for testing the possibility of analyzing SD images by modern computing systems in real-time. The main idea is to evaluate the performance of algorithms on images of actual size, excluding the reasons that may lead to a loss of tracking accuracy.

For the experiment, 15 anonymized video files were recorded from various ultrasound systems during radiofrequency ablation procedures – 8 men and 7 women aged 45 to 66 years. The following ultrasound systems were used:

1. GE Healthcare LOGIQ e
2. Philips iu22
3. BK Medical flexFocus 400

The duration of the files ranged from 20 to 30 seconds with a frame rate of 10-15 frames per second. So in each file there were from 260 to 430 SD-resolution frames. Their parameters are shown in the table below.

File name	Duration (sec)	FPS	Frames count	Resolution
1.avi	22	15	334	684*528
2.avi	20	15	304	684*528
3.avi	22	15	336	684*528
4.avi	24	15	364	684*528
5.avi	25	15	375	684*528
6.avi	28	10	281	800*600
7.avi	27	10	274	800*600
8.avi	28	10	281	800*600
9.avi	29	10	294	800*600
10.avi	26	10	264	800*600
11.avi	21	15	318	1020*818
12.avi	24	15	362	1020*818
13.avi	26	15	395	1020*818
14.avi	25	15	376	1020*818
15.avi	28	15	423	1020*818

Table 1. Video files specifications.

The experiment was planned as follows:

1. Preparation of anonymous video recordings.
2. Ground truth labeling.
3. Testing tracker algorithms for video recordings.
4. Analysis of the results.

A small software toolkit was created for the convenience of data processing with several utilities such as:

1. Video frames counter (experiments showed that the OpenCV library incorrectly determines the number of frames of an ASF-stream in a WMV container).

2. A module for saving a sequence of video frames to PNG image format (a format that allows storing video frames without further loss of quality).

3. A module for manual labeling reference areas and saving their coordinates.

The video preparation consisted of taking time-lapse images with the subsequent labeling of the zones to search for. Video frames with manually labeled search areas were taken as the reference coordinates of the neoplasms. Qualified oncologist surgeons have labeled them. Subsequently, these images were analyzed, and the area's coordinates were saved to a log file for the convenient analysis of the tracker’s experiment results.

Since the program for measuring the speed and quality of tracking processed frames works sequentially according to the "frame reading – tracking – data output" scheme. The number of frames per second in the internal representation of the video file did not correlate with the measured indicators since the new frame was processed only after the processing of the previous one had been completed.

Also, since the files were encoded using various codecs (Lagarith, Windows Media Video, etc.), only the time spent by the tracking procedure was considered.

The testing methodology included both quantitative (tracking time) and qualitative criteria of tracking algorithms:

1. Coverage – the main qualitative characteristic – is the ratio of the intersection of the found zone and the ground truth zone to their union **[30]**. In the case of the ideal operation of the algorithm, these areas will coincide. It is possible to estimate how much the search accuracy varies in percentage in other cases. The resulting value is in the segment [0; 1], which is from 0% to 100%, and the higher the value, the better it shows how much of the ground truth zone is covered by the tracking algorithm.

2. Centers Deviation (CD) – the distance in pixels between the center of the found zone and the center of the reference zone. A low value is better as it would precisely position the robotic arm.

3. False Positive Percentage (FPP) – the ratio of the found area located outside the ground truth to the whole found area. Allows to find out the percentage of false-positive information.

In addition, if the best algorithm fails on specific frames, the possibility of re-tracking this frame using another tracking algorithm was checked out **[31].**

All software was written in C++ in the Microsoft Visual Studio 2019 development environment.

Experiment

The experiment was carried out with the following hardware: CPU Intel Core i5-1035G1, RAM 16 GB. Operating system – Microsoft Windows 10 20H2 64-bits.

The results of the testing program are presented in the table below. A total of 4981 video frames were processed.

Tracker	Min time (ms)	Avg time (ms)	Max time (ms)	Success/Fails	Coverage (%)	CD (px)	FPP (%)
Boosting	22	31	63	4981 / 0	41.96	77	47.90
CSRT	28	35	47	4981 / 0	75.95	12	19.51
KCF	3	9	19	4893 / 88	81.72	10	12.57
MIL	2	3	6	2865 / 2116	54.72	73	38.74
MOSSE	38	60	78	4981 / 0	61.31	29	27.07
MedianFlow	1	1	2	3385 / 1596	50.88	22	40.46
TLD	39	71	109	4981 / 0	21.85	159	66.03

Table 2. Results of trackers testing.

Results and discussions. A visual inspection of the trackers' work during the testing process made it possible to determine potential favorites and possible outsiders. These ideas were confirmed due to the analysis of the obtained values.

Figure 2 shows the results of the algorithms processing the file 4.avi. The first frame of the video is on the left pane, frame #100 – in the middle, last frame #364 – on the right pane. All the algorithms started to work close to each other. However, after 100 frames, the TLD algorithm lost the reference zone, and its error increased by the end of the video series. In addition, the behavior of the CSRT algorithm is indicative – it is the one that managed to process all the frames of the experiment correctly. It tends to increase the search zone area, sometimes capturing excess. Still, at the same time, the centers of the reference and found zones do not diverge so much, which is essential when transferring data to the navigation system of a medical robot. The results of the other algorithms are very similar to each other.

Boosting – although this algorithm has never reported a negative tracking result, its final results aren't impressive – the reference zone is covered by less than 25%. In contrast, it has a significant area that is not related to the reference zone. Similar results are shown by the *MOSSE* and *TLD* algorithms – the coverage of the ground truth zone is on an average from 10% to 40%, and the area of the incorrectly defined tumor zone is comparable in size. At the same time, these two algorithms, similarly to Boosting, always report a successful search result. Besides, they are 2-2.5 times slower than Boosting on average. It can definitely be concluded that these algorithms are not suitable for solving the problem: both because of the low quality of the results and because of the constant result interpretation as successful.

MIL and *MedianFlow* algorithms generally showed similar results. In about 50% of cases, they reported the search failed – which the algorithms described above did not do. However, even in case of success, the area of correct coverage varied on average from 40% to 60% of ground truth area with a similar area of false-positive data. It is interesting to note the extremely high performance of these two algorithms – the average frame processing time was about 2 ms. This potentially makes it possible to achieve a video analysis speed exceeding several hundred frames per second in case of processing more suitable video.

KCF and *CSRT* lead this test, with an average coverage above 75% and false-positive results less than 15%. They also took the first two places for Distance between Centers Criterion.

Some of the frames that failed to process by the KCF algorithm are shown in Figure 3. CSRT processed all the frames correctly.

The average test results are shown in Figure 3. The first criterion – Coverage – displays how many percent on average the zone the algorithm finds covers the reference zone (the higher value, the better), and two leaders are apparent – the KCF and CSRT algorithms.

The second criterion – Distance between Centers – shows how far the average center of the reference zone and the center of the zone found by the algorithm are apart from each other. The closer these centers are located, the more accurately the tracking is made and makes it possible to transmit coordinates for the robotic arm more precisely. The previous two leaders have retained their positions.

The third criterion – False Positive Percentage – shows the ratio of the zone outside the reference to the total area of the zone found by the algorithm. It displays the percentage of false information that can lead to a loss of

positioning accuracy and should ideally tend to zero. The same leaders remained – KCF and CSRT.

The diagram in Figure 5 shows that KCF is the only the leader in quality testing; it has excellent speed results. It could make KCF the best choice for tracking lesions on ultrasound video, with the exception of some failed frames.

Conclusions

The CSRT and KCF algorithms are the leaders in this ranking. They always cover the target area at least 70%, and the average result is 80% or more. False-positive data does not exceed 20% for CSRT and 15% for KCF. The speed of the CSRT algorithm allows it to reach 30 frames per second and KCF – up to 100 frames per second which makes them suitable for real-time processing. The failure rate for the KCF algorithm is less than 2%. With CSRT – all attempts were successful.

The reason for the failures of the other algorithms can be a whole complex of features of the ultrasound image, such as:

- noisy image,
- the absence of clearly defined contours of objects,
- gray-scale representation.

The obtained results led to the idea of cooperative use of algorithms: to build a reliable tracking system, it is proposed to use Kernelized Correlation Filters as the main algorithm and in rare cases of its failure to call the Channel Spatial Reliability algorithm, which, despite the lower operation speed, will eliminate dropped frames. The workflow might look like this:

1. Sequential processing of video frames using the KCF tracker.

2. If the KCF tracker fails, the CSRT algorithm is reinitialized with the last successful processed frame and repeats the search on the frame that caused the failure.

3. If step 2 is repeated several (supposedly 3-5 frames) times, the main KCF algorithm is reinitialized with the data received from the backup CSRT tracker.

4. Probably, it makes sense to go to step 2 in case of failure and when the arithmetic means of the distance according to CD criterion exceeds a certain predetermined threshold and/or the value of Coverage criterion exceeds the value of FPP criterion.

Thus, the conclusion of the work suggests that real-time neoplasm tracking is possible using a combination of the two algorithms. This will allow the system to reliably track target areas at frame rates in excess of 50 frames per second. Such development will be future work for this group of authors.

References

1. Grazioli L, Ambrosini R, Frittoli B, Grazioli M, Morone M. Primary benign liver lesions. Eur J Radiol. 2017 Oct;95:378-398. doi: 10.1016/j.ejrad.2017.08.028. Epub 2017 Sep 1. PMID: 28987695.

2. Furlan A, Marin D, Bae KT, Lagalla R, Agnello F, Bazzocchi M, Brancatelli G. Focal liver lesions hyperintense on T1-weighted magnetic resonance images. Semin Ultrasound CT MR. 2009 Oct;30(5):436-49. doi: 10.1053/j.sult.2009.07.002. PMID: 19842568.
3. Cogley JR, Miller FH. MR imaging of benign focal liver lesions. Radiol Clin North Am. 2014 Jul;52(4):657-82. doi: 10.1016/j.rcl.2014.02.005. Epub 2014 Apr 4. PMID: 24889166.
4. Brannigan M, Burns PN, Wilson SR. Blood flow patterns in focal liver lesions at microbubble-enhanced US. Radiographics. 2004 Jul-Aug;24(4):921-35. doi: 10.1148/rg.244035158. PMID: 15256618.
5. Reid-Lombardo KM, Khan S, Sclabas G. Hepatic cysts and liver abscess. Surg Clin North Am. 2010 Aug;90(4):679-97. doi: 10.1016/j.suc.2010.04.004. PMID: 20637941.
6. Siegel RL, Miller KD, Jemal A. Cancer statistics, 2020. CA Cancer J Clin. 2020 Jan;70(1):7-30. doi: 10.3322/caac.21590. Epub 2020 Jan 8. PMID: 31912902.
7. Arnold M, Sierra MS, Laversanne M, Soerjomataram I, Jemal A, Bray F. Global patterns and trends in colorectal cancer incidence and mortality. Gut. 2017 Apr;66(4):683-691. doi: 10.1136/gutjnl-2015-310912. Epub 2016 Jan 27. PMID: 26818619.
8. Jim MA, Pinheiro PS, Carreira H, Espey DK, Wiggins CL, Weir HK. Stomach cancer survival in the United States by race and stage (2001-2009): Findings from the CONCORD-2 study. Cancer. 2017 Dec 15;123 Suppl 24(Suppl 24):4994-5013. doi: 10.1002/cncr.30881. PMID: 29205310; PMCID: PMC5826592.
9. Qiu MZ, Shi SM, Chen ZH, Yu HE, Sheng H, Jin Y, Wang DS, Wang FH, Li YH, Xie D, Zhou ZW, Yang DJ, Xu RH. Frequency and clinicopathological features of metastasis to liver, lung, bone, and brain from gastric cancer: A SEER-based study. Cancer Med. 2018 Aug;7(8):3662-3672. doi: 10.1002/cam4.1661. Epub 2018 Jul 9. PMID: 29984918; PMCID: PMC6089142.
10. Horn SR, Stoltzfus KC, Lehrer EJ, Dawson LA, Tchelebi L, Gusani NJ, Sharma NK, Chen H, Trifiletti DM, Zaorsky NG. Epidemiology of liver metastases. Cancer Epidemiol. 2020 Aug;67:101760. doi: 10.1016/j.canep.2020.101760. Epub 2020 Jun 17. PMID: 32562887.
11. Veldkamp R, Kuhry E, Hop WC, Jeekel J, Kazemier G, Bonjer HJ, Haglind E, Påhlman L, Cuesta MA, Msika S, Morino M, Lacy AM; COlon cancer Laparoscopic or Open Resection Study Group (COLOR). Laparoscopic surgery versus open surgery for colon cancer: short-term outcomes of a randomised trial. Lancet Oncol. 2005 Jul;6(7):477-84. doi: 10.1016/S1470-2045(05)70221-7. PMID: 15992696.
12. Levin AA, Klimov DD, Nechunaev AA, Vorotnikov AA, Prokhorenko LS, Grigorieva EV, Astakhov DA, Poduraev YV, Panchenkov DN. The comparison of the process of manual and robotic positioning of the electrode performing radiofrequency ablation under the control of a surgical navigation system. Sci Rep. 2020 May 25;10(1):8612. doi: 10.1038/s41598-020-64472-9. PMID: 32451395; PMCID: PMC7248067.
13. Zhou Z, Wu W, Wu S, Tsui PH, Lin CC, Zhang L, Wang T. Semi-automatic breast ultrasound image segmentation based on mean shift and graph cuts. Ultrason Imaging. 2014 Oct;36(4):256-76. doi: 10.1177/0161734614524735. Epub 2014 Apr 22. PMID: 24759696.
14. Shengfeng Liu, Yi Wang, Xin Yang, Baiying Lei, Li Liu, Shawn Xiang Li, Dong Ni, Tianfu Wang, Deep Learning in Medical Ultrasound Analysis: A Review, Engineering, Volume 5, Issue 2, 2019, Pages 261-275, ISSN 2095-8099, https://doi.org/10.1016/j.eng.2018.11.020.
15. Lee MW, Kim YJ, Park HS, Yu NC, Jung SI, Ko SY, Jeon HJ. Targeted sonography for small hepatocellular carcinoma discovered by CT or MRI: factors affecting sonographic detection. AJR Am J Roentgenol. 2010 May;194(5):W396-400. doi: 10.2214/AJR.09.3171. PMID: 20410384.

16. Vorotnikov AA, Klimov DD, Melnichenko EA, Poduraev YV, Bazykyan EA. Criteria for comparison of robot movement trajectories and manual movements of a doctor for performing maxillofacial surgeries. International Journal of Mechanical Engineering and Robotics Research 2018, 7(4), 361–366. https://doi.org/10.18178/ijmerr.7.4.361-366
17. Ahmed M, Solbiati L, Brace CL, Breen DJ, Callstrom MR, Charboneau JW, Chen MH, Choi BI, de Baère T, Dodd GD 3rd, Dupuy DE, Gervais DA, Gianfelice D, Gillams AR, Lee FT Jr, Leen E, Lencioni R, Littrup PJ, Livraghi T, Lu DS, McGahan JP, Meloni MF, Nikolic B, Pereira PL, Liang P, Rhim H, Rose SC, Salem R, Sofocleous CT, Solomon SB, Soulen MC, Tanaka M, Vogl TJ, Wood BJ, Goldberg SN; International Working Group on Image-guided Tumor Ablation; Interventional Oncology Sans Frontières Expert Panel; Technology Assessment Committee of the Society of Interventional Radiology,; Standard of Practice Committee of the Cardiovascular and Interventional Radiological Society of Europe. Image-guided tumor ablation: standardization of terminology and reporting criteria–a 10-year update. Radiology. 2014 Oct;273(1):241-60. doi: 10.1148/radiol.14132958. Epub 2014 Jun 13. PMID: 24927329; PMCID: PMC4263618.
18. Alkhatib M, Hafiane A, Tahri O, Vieyres P, Delbos A. Adaptive median binary patterns for fully automatic nerves tracking in ultrasound images. Comput Methods Programs Biomed. 2018 Jul;160:129-140. doi: 10.1016/j.cmpb.2018.03.013. Epub 2018 Mar 21. PMID: 29728240.
19. http://cvlab.hanyang.ac.kr/tracker_benchmark/datasets.html
20. https://github.com/opencv/opencv
21. https://github.com/opencv/opencv_contrib
22. Grabner Helmut, Grabner Michael, Bischof Horst. (2006). Real-Time Tracking via On-line Boosting. Proceedings of British Machine Vision Conference (BMVC). 1. 47-56. 10.5244/C.20.6.
23. Babenko Boris, Yang Ming-Hsuan, Belongie Serge. (2009). Visual tracking with online Multiple Instance Learning. Proceedings / CVPR, IEEE Computer Society Conference on Computer Vision and Pattern Recognition. IEEE Computer Society Conference on Computer Vision and Pattern Recognition. 983-990. 10.1109/CVPR.2009.5206737.
24. Nedzvedz Olga, Jin Luhong, Nedzved Alexander, Lin Wanni, Ablameyko Sergey, Xu, Yingke. (2019). Automatic Analysis of Moving Particles by Total Internal Reflection Fluorescence Microscopy. Communications in Computer and Information Science. 1055. 228-239. 10.1007/978-3-030-35430-5_19.
25. Lukezic Alan, Tomas Vojir, Luka Cehovin, Jiri Matas and Matej Kristan. “Discriminative Correlation Filter with Channel and Spatial Reliability.” ArXiv abs/1611.08461 (2017): n. pag.
26. Bolme David, Beveridge J., Draper Bruce, Lui, Yui. (2010). Visual object tracking using adaptive correlation filters. Proceedings of the IEEE Computer Society Conference on Computer Vision and Pattern Recognition. 2544-2550. 10.1109/CVPR.2010.5539960.
27. Zdenek Kalal, Krystian Mikolajczyk and Jiri Matas. "Forward-Backward Error: Automatic Detection of Tracking Failures." Paper presented at the meeting of the ICPR, 2010.
28. Zdenek Kalal, Krystian Mikolajczyk, and Jiri Matas "Tracking-Learning- Detection" IEEE TRANSACTIONS ON PATTERN ANALYSIS AND MACHINE INTELLIGENCE, VOL. 34
29. Huang P, Su L, Chen S, Cao K, Song Q, Kazanzides P, Iordachita I, Lediju Bell MA, Wong JW, Li D, Ding K. 2D ultrasound imaging based intra-fraction respiratory motion tracking for abdominal radiation therapy using machine learning. Phys Med Biol. 2019 Sep 11;64(18):185006. doi: 10.1088/1361-6560/ab33db. PMID: 31323649.

30. De Luca V, Benz T, Kondo S, König L, Lübke D, Rothlübbers S, Somphone O, Allaire S, Lediju Bell MA, Chung DY, Cifor A, Grozea C, Günther M, Jenne J, Kipshagen T, Kowarschik M, Navab N, Rühaak J, Schwaab J, Tanner C. The 2014 liver ultrasound tracking benchmark. Phys Med Biol. 2015 Jul 21;60(14):5571-99. doi: 10.1088/0031-9155/60/14/5571. Epub 2015 Jul 2. PMID: 26134417; PMCID: PMC5454593.
31. Peter Janku, Karel Koplik, Tomas Dulik, Istvan Szabo. (2016). Comparison of tracking algorithms implemented in OpenCV. MATEC Web of Conferences. 76. 04031. 10.1051/matecconf/20167604031.
32. Suryansh Pratap Singh, Akshat Mittal, Manas Gupta, Soumalya Ghosh, Anupam Lakhanpale. (2021). Comparing Various Tracking Algorithms In OpenCV. Turkish Journal of Computer and Mathematics Education Vol.12 No.6 (2021), 5193-5198.

Declarations

Acknowledgements.

This study was supported by the Ministry of Health of the Russian Federation in the framework of the State Contract No. 056-00035-21-00 of December 17, 2020.

Author contributions.

Poduraev Y.V., Panchenkov D.N. and Klimov D.D. developed the concept of the work. Klimov D.D., Mishchenkov D.S., Prokhorenko L.S. and Levin A.A. conceived and planned the experiment. Klimov D.D. and Levin A.A. developed the software for the experiment. Klimov D.D., Mishchenkov D.S. and Prokhorenko L.S. carried out the experiment. Nosova A.G., Nechunaev A.A. and Astakhov D.A. performed US data collection, analysis, labeling and interpretation. Levin A.A., Klimov D.D., and Nechunaev A.A. wrote the main manuscript text and prepared all Figures and Tables. All authors provided critical feedback and helped shape the research, analysis, and manuscript. Nosova A.G. and Astakhov D.A. performed critical revision of the article. Poduraev Y.V. and Panchenkov D.N. performed final approval of the version to be published.

Competing interests.

There is potential Competing Interest. Support by the Ministry of Health of the Russian Federation in the framework of the State Contract No. 056-00035-21-00 of December 17, 2020.

Figures

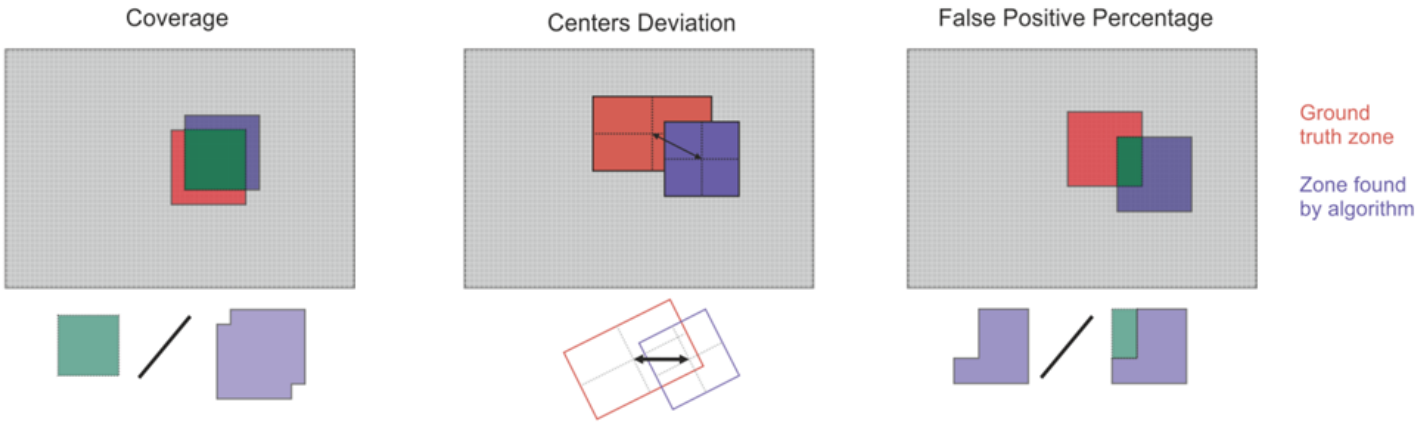

Figure 1

Criteria visual representation.

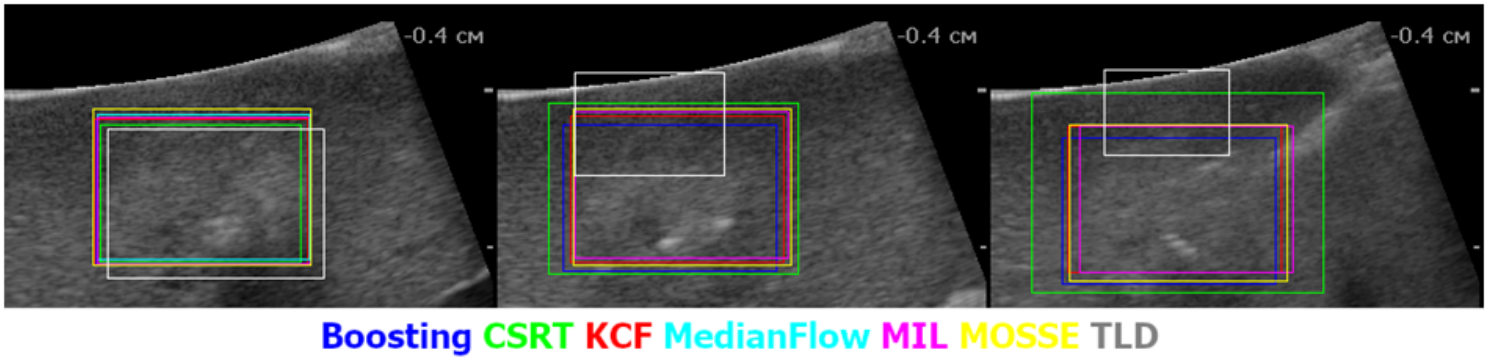

Figure 2

Example of trackers testing.

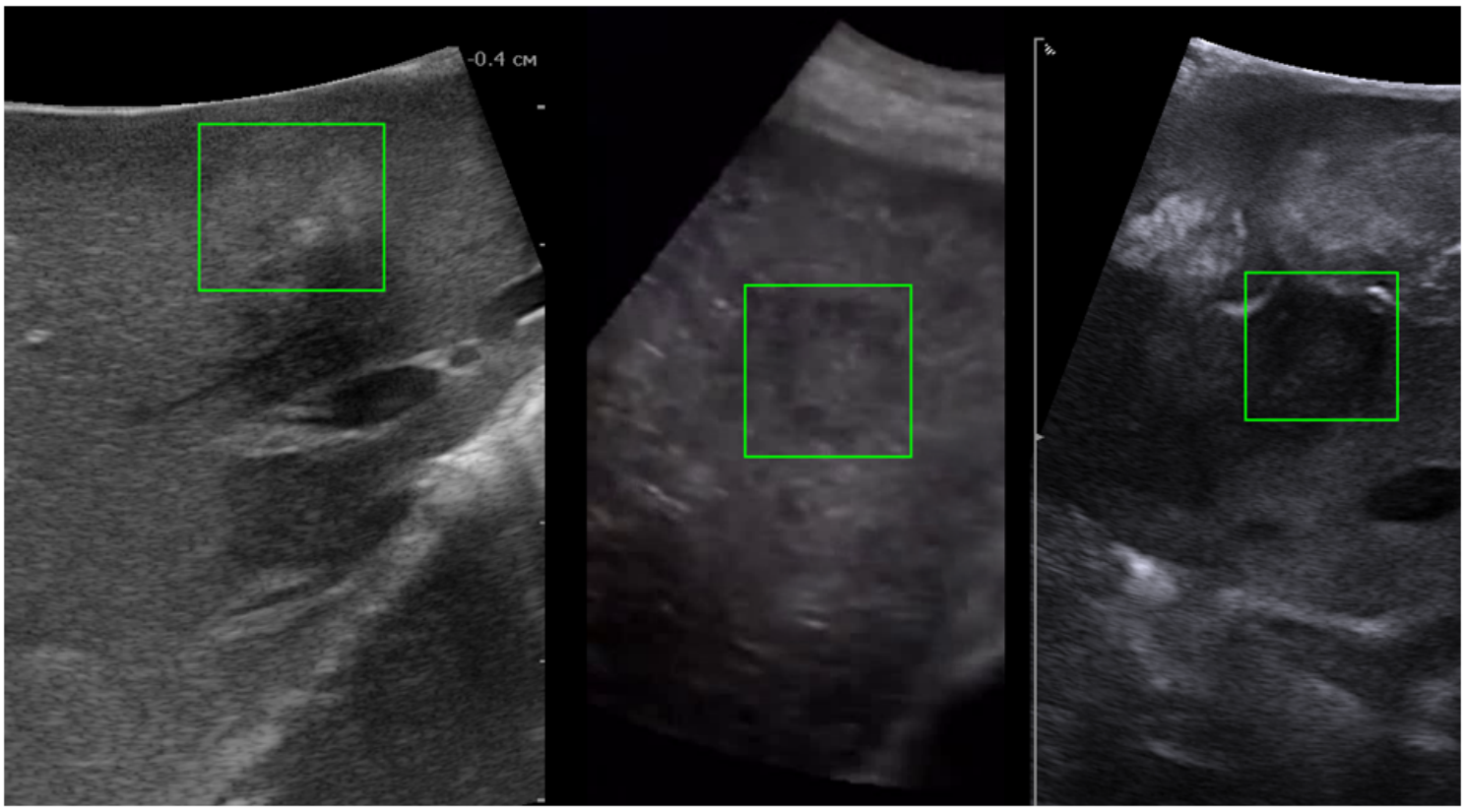

Figure 3

Several frames failed by KCF (Ground truth zone is green).

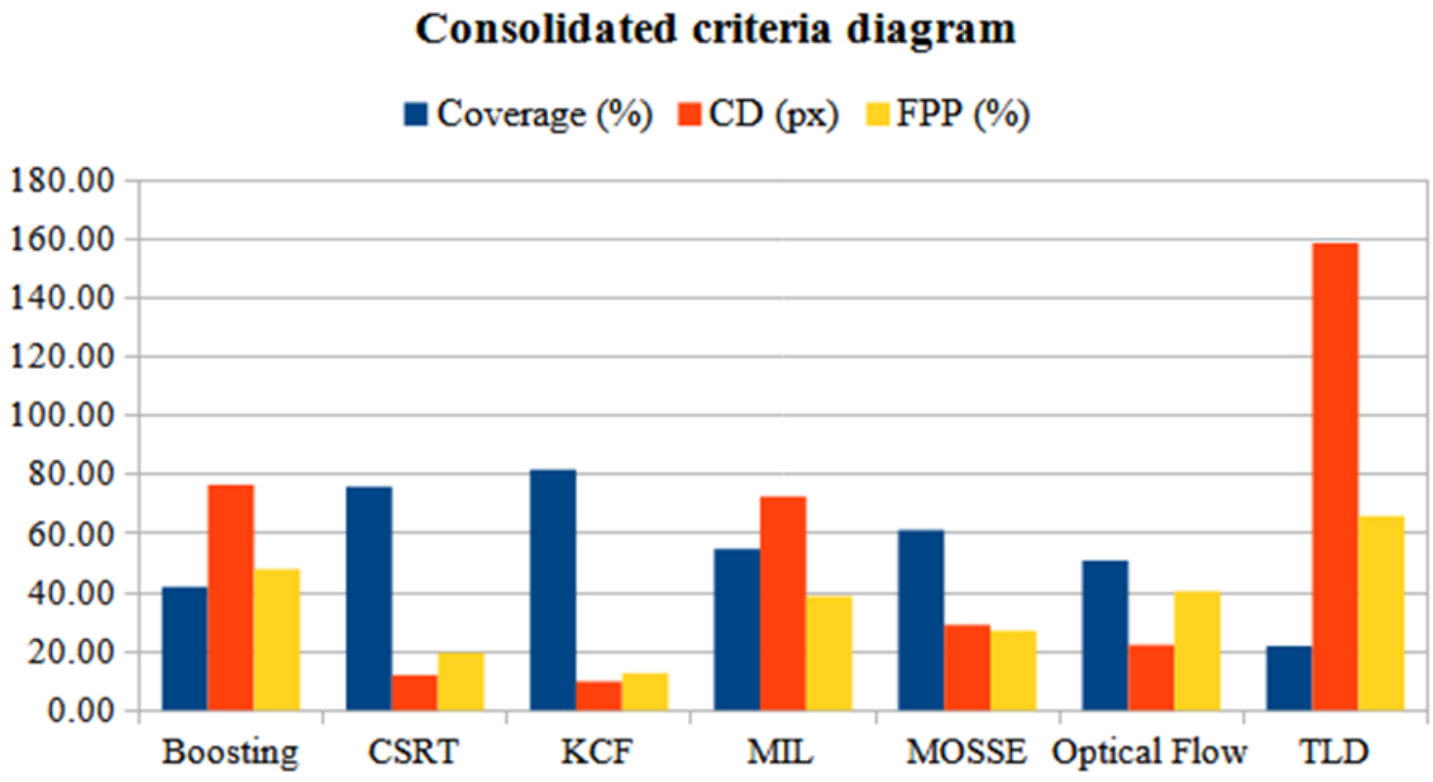

Figure 4

Consolidated results.

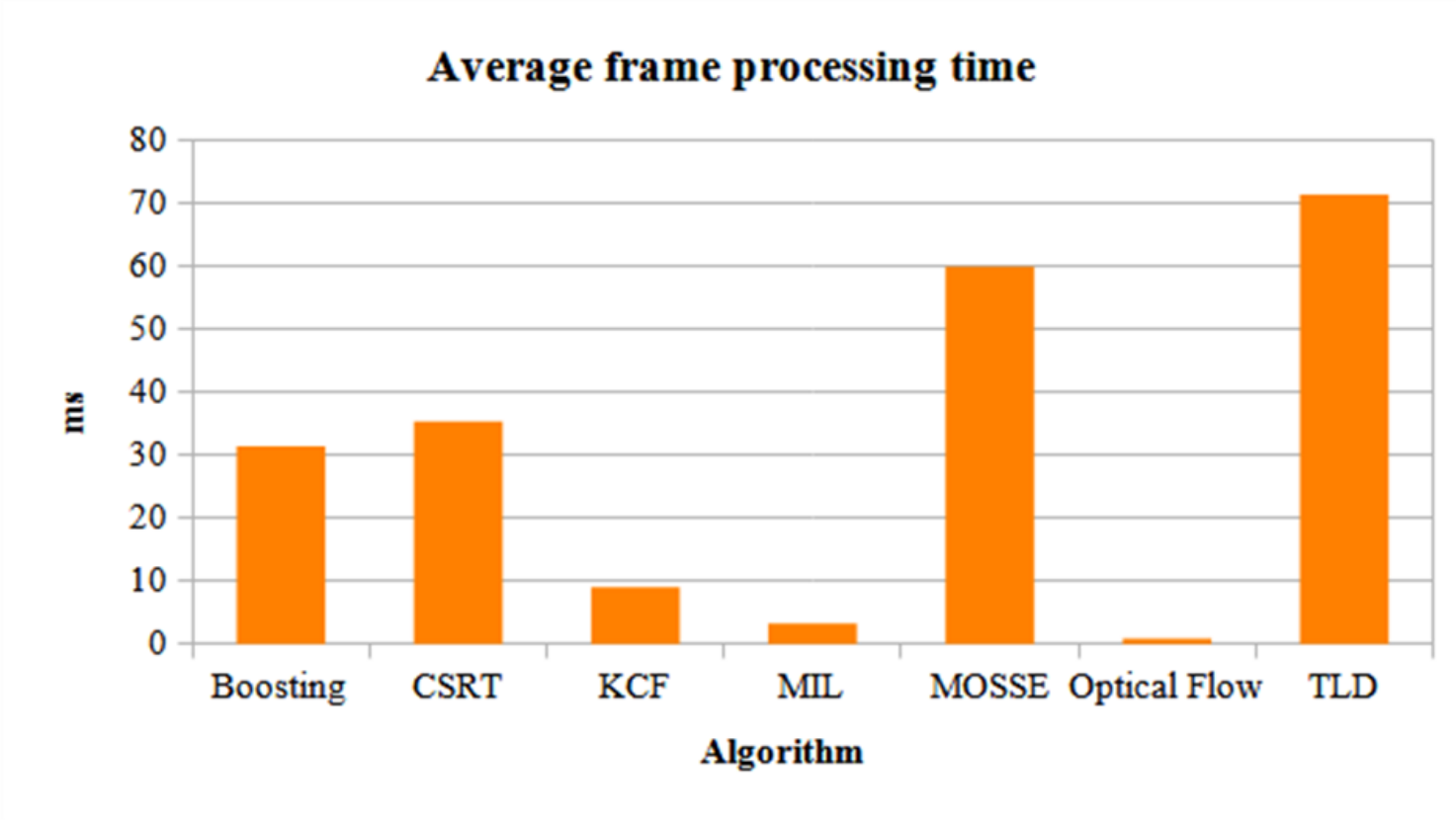

Figure 5

Average frame processing time.